

Search for $D^0\text{-}\bar{D}^0$ Mixing

R. Godang,¹ K. Kinoshita,^{1*} I. C. Lai,¹ S. Schrenk,¹ G. Bonvicini,² D. Cinabro,² L. P. Perera,² G. J. Zhou,² G. Eigen,³ E. Lipeles,³ M. Schmidler,³ A. Shapiro,³ W. M. Sun,³ A. J. Weinstein,³ F. Würthwein,^{3,†} D. E. Jaffe,⁴ G. Masek,⁴ H. P. Paar,⁴ E. M. Potter,⁴ S. Prell,⁴ V. Sharma,⁴ D. M. Asner,⁵ A. Eppich,⁵ J. Gronberg,⁵ T. S. Hill,⁵ C. M. Korte,⁵ R. Kutschke,⁵ D. J. Lange,⁵ R. J. Morrison,⁵ H. N. Nelson,⁵ C. Qiao,⁵ A. Ryd,⁵ H. Tajima,⁵ M. S. Witherell,⁵ R. A. Briere,⁶ B. H. Behrens,⁷ W. T. Ford,⁷ A. Gritsan,⁷ J. Roy,⁷ J. G. Smith,⁷ J. P. Alexander,⁸ R. Baker,⁸ C. Bebek,⁸ B. E. Berger,⁸ K. Berkelman,⁸ F. Blanc,⁸ V. Boisvert,⁸ D. G. Cassel,⁸ M. Dickson,⁸ P. S. Drell,⁸ K. M. Ecklund,⁸ R. Ehrlich,⁸ A. D. Foland,⁸ P. Gaidarev,⁸ L. Gibbons,⁸ B. Gittelman,⁸ S. W. Gray,⁸ D. L. Hartill,⁸ B. K. Heltsley,⁸ P. I. Hopman,⁸ C. D. Jones,⁸ N. Katayama,⁸ D. L. Kreinick,⁸ M. Lohner,⁸ A. Magerkurth,⁸ T. O. Meyer,⁸ N. B. Mistry,⁸ C. R. Ng,⁸ E. Nordberg,⁸ J. R. Patterson,⁸ D. Peterson,⁸ D. Riley,⁸ J. G. Thayer,⁸ P. G. Thies,⁸ B. Valant-Spaight,⁸ A. Warburton,⁸ P. Avery,⁹ C. Prescott,⁹ A. I. Rubiera,⁹ J. Yelton,⁹ J. Zheng,⁹ G. Brandenburg,¹⁰ A. Ershov,¹⁰ Y. S. Gao,¹⁰ D. Y.-J. Kim,¹⁰ R. Wilson,¹⁰ T. E. Browder,¹¹ Y. Li,¹¹ J. L. Rodriguez,¹¹ H. Yamamoto,¹¹ T. Bergfeld,¹² B. I. Eisenstein,¹² J. Ernst,¹² G. E. Gladding,¹² G. D. Gollin,¹² R. M. Hans,¹² E. Johnson,¹² I. Karliner,¹² M. A. Marsh,¹² M. Palmer,¹² C. Plager,¹² C. Sedlack,¹² M. Selen,¹² J. J. Thaler,¹² J. Williams,¹² K. W. Edwards,¹³ R. Janicek,¹⁴ P. M. Patel,¹⁴ A. J. Sadoff,¹⁵ R. Ammar,¹⁶ A. Bean,¹⁶ D. Besson,¹⁶ R. Davis,¹⁶ I. Kravchenko,¹⁶ N. Kwak,¹⁶ X. Zhao,¹⁶ S. Anderson,¹⁷ V. V. Frolov,¹⁷ Y. Kubota,¹⁷ S. J. Lee,¹⁷ R. Mahapatra,¹⁷ J. J. O'Neill,¹⁷ R. Poling,¹⁷ T. Riehle,¹⁷ A. Smith,¹⁷ J. Urheim,¹⁷ S. Ahmed,¹⁸ M. S. Alam,¹⁸ S. B. Athar,¹⁸ L. Jian,¹⁸ L. Ling,¹⁸ A. H. Mahmood,^{18,‡} M. Saleem,¹⁸ S. Timm,¹⁸ F. Wappler,¹⁸ A. Anastassov,¹⁹ J. E. Duboscq,¹⁹ K. K. Gan,¹⁹ C. Gwon,¹⁹ T. Hart,¹⁹ K. Honscheid,¹⁹ D. Hufnagel,¹⁹ H. Kagan,¹⁹ R. Kass,¹⁹ T. K. Pedlar,¹⁹ H. Schwarthoff,¹⁹ J. B. Thayer,¹⁹ E. von Toerne,¹⁹ M. M. Zoeller,¹⁹ S. J. Richichi,²⁰ H. Severini,²⁰ P. Skubic,²⁰ A. Undrus,²⁰ S. Chen,²¹ J. Fast,²¹ J. W. Hinson,²¹ J. Lee,²¹ N. Menon,²¹ D. H. Miller,²¹ E. I. Shibata,²¹ I. P. J. Shipsey,²¹ V. Pavlunin,²¹ D. Cronin-Hennessy,²² Y. Kwon,^{22,§} A. L. Lyon,²² E. H. Thorndike,²² C. P. Jessop,²³ H. Marsiske,²³ M. L. Perl,²³ V. Savinov,²³ D. Ugolini,²³ X. Zhou,²³ T. E. Coan,²⁴ V. Fadeyev,²⁴ Y. Maravin,²⁴ I. Narsky,²⁴ R. Stroynowski,²⁴ J. Ye,²⁴ T. Wlodek,²⁴ M. Artuso,²⁵ R. Ayad,²⁵ C. Boulahouache,²⁵ K. Bukin,²⁵ E. Dambasuren,²⁵ S. Karamov,²⁵ S. Kopp,²⁵ G. Majumder,²⁵ G. C. Moneti,²⁵ R. Mountain,²⁵ S. Schuh,²⁵ T. Skwarnicki,²⁵ S. Stone,²⁵ G. Viehhauser,²⁵ J. C. Wang,²⁵ A. Wolf,²⁵ J. Wu,²⁵ S. E. Csorna,²⁶ I. Danko,²⁶ K. W. McLean,²⁶ Sz. Márka,²⁶ and Z. Xu²⁶

(CLEO Collaboration)

¹Virginia Polytechnic Institute and State University, Blacksburg, Virginia 24061

²Wayne State University, Detroit, Michigan 48202

³California Institute of Technology, Pasadena, California 91125

⁴University of California, San Diego, La Jolla, California 92093

⁵University of California, Santa Barbara, California 93106

⁶Carnegie Mellon University, Pittsburgh, Pennsylvania 15213

⁷University of Colorado, Boulder, Colorado 80309-0390

⁸Cornell University, Ithaca, New York 14853

⁹University of Florida, Gainesville, Florida 32611

¹⁰Harvard University, Cambridge, Massachusetts 02138

¹¹University of Hawaii at Manoa, Honolulu, Hawaii 96822

¹²University of Illinois, Urbana-Champaign, Illinois 61801

¹³Carleton University, Ottawa, Ontario, Canada K1S 5B6

and the Institute of Particle Physics, Canada

¹⁴McGill University, Montréal, Québec, Canada H3A 2T

and the Institute of Particle Physics, Canada

¹⁵Ithaca College, Ithaca, New York 14850

¹⁶University of Kansas, Lawrence, Kansas 66045

¹⁷University of Minnesota, Minneapolis, Minnesota 55455

¹⁸State University of New York at Albany, Albany, New York 12222

¹⁹The Ohio State University, Columbus, Ohio 43210

²⁰University of Oklahoma, Norman, Oklahoma 73019

²¹Purdue University, West Lafayette, Indiana 47907

²²University of Rochester, Rochester, New York 14627

²³Stanford Linear Accelerator Center, Stanford University, Stanford, California 94309

²⁴Southern Methodist University, Dallas, Texas 75275

²⁵Syracuse University, Syracuse, New York 13244²⁶Vanderbilt University, Nashville, Tennessee 37235

(Received 3 January 2000)

We have studied the “wrong-sign” process $D^0 \rightarrow K^+ \pi^-$ to search for D^0 - \bar{D}^0 mixing. The data come from 9.0 fb^{-1} of e^+e^- collisions at $\sqrt{s} \approx 10 \text{ GeV}$ recorded with the CLEO II.V detector. We measure the relative rate of the wrong-sign process $D^0 \rightarrow K^+ \pi^-$ to the Cabibbo-favored process $\bar{D}^0 \rightarrow K^+ \pi^-$ to be $R = (0.332^{+0.063}_{-0.065} \pm 0.040)\%$. We study $D^0 \rightarrow K^+ \pi^-$ as a function of decay time to distinguish direct doubly Cabibbo-suppressed decay from D^0 - \bar{D}^0 mixing. The amplitudes that describe D^0 - \bar{D}^0 mixing, x' and y' , are consistent with zero. At the 95% C.L. and without assumptions concerning charge-parity (CP) violating parameters, we find $(1/2)x'^2 < 0.041\%$ and $-5.8\% < y' < 1.0\%$.

PACS numbers: 13.25.Ft, 12.15.Mm, 14.40.Lb

Studies of the evolution of a K^0 or B_d^0 into the respective antiparticle, a \bar{K}^0 or \bar{B}_d^0 , have guided the form and content of the standard model and permitted useful estimates of the masses of the charm and top quark prior to their direct observation [1]. In this Letter, we present the results of a search for the evolution of the D^0 into the \bar{D}^0 . Our principal motivation is to observe new physics outside the standard model.

A D^0 can evolve into a \bar{D}^0 through on-shell intermediate states, such as K^+K^- with mass, $m_{K^+K^-} = m_{D^0}$, or through off-shell intermediate states, such as those that might be present due to new physics. We denote the amplitude through the former (later) states by $-iy(x)$, in units of $\Gamma_{D^0}/2$ [2]. Many predictions for x in the $D^0 \rightarrow \bar{D}^0$ amplitude have been made [3]. The standard model contributions are suppressed to $|x| \approx \tan^2 \theta_C \approx 5\%$ because D^0 decay is Cabibbo-favored; the Glashow-Illiopolous-Maiani [4] cancellation could further suppress $|x|$ down to 10^{-6} – 10^{-2} . Many non-standard models predict $|x| > 1\%$. Contributions to x at this level could result from the presence of new particles with masses as high as 100–1000 TeV [5]. Signatures of new physics include $|x| \gg |y|$, or charge-parity (CP) violating interference between x and y , or between x and a direct decay amplitude. In order to assess the origin of a D^0 - \bar{D}^0 mixing signal, the effects described by y must be distinguished from those described by x .

The wrong-sign (WS) process, $D^0 \rightarrow K^+ \pi^-$, can proceed either through direct doubly Cabibbo-suppressed decay (DCSD) or through state mixing followed by the Cabibbo-favored decay (CFD), $D^0 \rightarrow \bar{D}^0 \rightarrow K^+ \pi^-$. Both processes could contribute to the time integrated WS rate $R = (f + \bar{f})/2$, and the inclusive CP asymmetry $A = (f - \bar{f})/(f + \bar{f})$, where $f = \Gamma(D^0 \rightarrow K^+ \pi^-)/\Gamma(\bar{D}^0 \rightarrow K^+ \pi^-)$, and \bar{f} is defined by the application of charge conjugation to f .

To disentangle the processes that could contribute to $D^0 \rightarrow K^+ \pi^-$, we study the distribution of WS final states as a function of the proper decay time t of the D^0 . We describe the proper decay time in units of the mean D^0 lifetime, $\tau_{D^0} = 415 \pm 4 \text{ fs}$ [6]. The differential WS rate relative to the right-sign (RS) process, $\bar{D}^0 \rightarrow K^+ \pi^-$ is [7]

$$r(t) \equiv \left[R_D + \sqrt{R_D} y' t + \frac{1}{4} (x'^2 + y'^2) t^2 \right] e^{-t}. \quad (1)$$

The modified mixing amplitudes x' and y' in Eq. (1) are given by $y' \equiv y \cos \delta - x \sin \delta$ and $x' \equiv x \cos \delta + y \sin \delta$, where δ is a possible strong phase between the DCSD and CFD amplitudes; there are theoretical arguments that δ is small [8]. The coefficient of the term quadratic in t is proportional to the relative rate of mixing $R_M \equiv \frac{1}{2}(x^2 + y^2) = \frac{1}{2}(x'^2 + y'^2)$. The relative rate of DCSD is R_D .

The influence of each of x' , y' , and R_D on $r(t)$ in Eq. (1) is distinguishable. Such behavior is complementary to the time dependence of the decay rate to CP eigenstates such as $D^0 \rightarrow K^+ K^-$ that is primarily sensitive to y , or that of $D^0 \rightarrow K^+ \ell^- \bar{\nu}_\ell$ that is sensitive to R_M alone.

We characterize the violation of CP in state mixing, direct decay, and the interference between those two processes, respectively, by the real-valued parameters A_M , A_D , and ϕ , where, to leading order, both x' and y' are scaled by $(1 \pm A_M)^{\frac{1}{2}}$, $R_D \rightarrow R_D(1 \pm A_D)$, $\delta \rightarrow \delta \pm \phi$ in Eq. (1) [9]. The plus (minus) sign is used for an initial D^0 (\bar{D}^0).

Our data were accumulated between February 1996 and February 1999 from an integrated luminosity of 9.0 fb^{-1} of e^+e^- collisions at $\sqrt{s} \approx 10 \text{ GeV}$ provided by the Cornell Electron Storage Ring (CESR). The data were taken with the CLEO II multipurpose detector [10], upgraded in 1995 when a silicon vertex detector (SVX) was installed [11] and the drift chamber gas was changed from argon-ethane to helium-propane. The upgraded configuration is named CLEO II.V.

We reconstruct candidates for the decay sequence $D^{*+} \rightarrow \pi_s^+ D^0$, $D^0 \rightarrow K^\pm \pi^\mp$. The charge of the slow pion (π_s^+ or π_s^-) identifies the charm state at $t = 0$ as either D^0 or \bar{D}^0 . We require the D^{*+} momentum, p_{D^*} , to exceed 2.2 GeV, and we require the D^0 to produce either the final state $K^+ \pi^-$ (WS) or $K^- \pi^+$ (RS). The broad features of the reconstruction are similar to those employed in the recent CLEO measurement of the D meson lifetimes [12].

The SVX provides precise measurement of the charged particle trajectories, or “tracks,” in three dimensions. We

are thus able to refit the K^+ and π^- tracks with a requirement that they form a common vertex in three dimensions and require that the confidence level (C.L.) of the refit exceed 0.01%. We use the trajectory of the $K^+\pi^-$ system and the position of the CESR luminous region to obtain the D^0 production point. We refit the π_s^+ track with a requirement that the trajectory intersect the D^0 production point and require that the confidence level of the refit exceed 0.01%.

We reconstruct the energy released in the $D^{*+} \rightarrow \pi_s^+ D^0$ decay as $Q \equiv M^* - M - m_\pi$, where M^* is the reconstructed mass of the $\pi_s^+ K^+ \pi^-$ system, M is the reconstructed mass of the $K^+ \pi^-$ system, and m_π is the charged pion mass. The addition of the D^0 production point to the π_s^+ trajectory, as well as track-fitting improvements, yields the resolution $\sigma_Q = 190 \pm 2$ keV [13]. The use of helium-propane, in addition to improvements in track fitting, yields the resolution $\sigma_M = 6.4 \pm 0.1$ MeV [13]. Candidates with poorly reconstructed Q or M are rejected. These resolutions are better than those of earlier studies [14–17] and permit improved suppression of background processes.

Candidates must pass two kinematic requirements designed to suppress backgrounds from $D^0 \rightarrow \pi^+ \pi^-$, $D^0 \rightarrow K^+ K^-$, $D^0 \rightarrow$ multibody, and from cross feed between WS and RS decays. We evaluate the mass M for $D^0 \rightarrow K^+ \pi^-$ candidates under the three alternate hypotheses $D^0 \rightarrow \pi^+ \pi^-$, $D^0 \rightarrow K^+ K^-$, and $D^0 \rightarrow \pi^+ K^-$. If any one of the three masses falls within 4σ , computed from the covariance matrices of the fit, of the D^0 mass [6], the $D^0 \rightarrow K^+ \pi^-$ candidate is rejected. A conjugate requirement is made for the RS decays. The second kinematic requirement rejects asymmetric D^0 decays where the pion candidate has low momentum with the requirement that $\cos\theta^* > -0.8$ where θ^* is the angle of the pion candidate in the D^0 rest frame with respect to the D^0 boost. The relative efficiency for the CFD to pass the two kinematic requirements is 84% and 91%, respectively.

We reconstruct t using only the vertical (y) component of the flight distance of the D^0 candidate. This reconstruction is effective because the vertical extent of the e^+e^- luminous region has $\sigma_y = 7 \mu\text{m}$ [18]. The resolution on the D^0 decay point (x_v, y_v, z_v) is typically $40 \mu\text{m}$ in each dimension. We measure the centroid of the luminous region (x_b, y_b, z_b) with hadronic events in blocks of data with integrated luminosities of several pb^{-1} , and an error on y_b that is less than $5 \mu\text{m}$. We reconstruct t as $t = M/p_y \times (y_v - y_b)/(c\tau_{D^0})$, where p_y is the y component of the total momentum of the $K^+ \pi^-$ system. The error in t , σ_t , is typically 0.4 (in D^0 lifetimes), although when the D^0 direction is near the horizontal plane, σ_t can be large; we require $\sigma_t < 3/2$, which rejects 12% of the signal, measured with the CFD. Studies of the plentiful RS sample allow us to determine our resolution function [12] and show that biases are negligible for the WS results.

Our signal for the WS process $D^0 \rightarrow K^+ \pi^-$ is shown in Fig. 1. We determine the background levels by performing a fit to the two-dimensional region of $0 < Q < 10$ MeV versus $1.76 < M < 1.97$ GeV that has an area 135 times larger than our signal region. Event samples generated by the Monte Carlo (MC) method and fully simulated in our detector [19] corresponding to 90 fb^{-1} of integrated luminosity are used to estimate the background shapes in the Q - M plane. The normalizations of the background components with distinct distributions in the Q - M plane are allowed to vary in the fit to the data. The background distributions and normalizations in the D^0 and \bar{D}^0 samples are consistent and constrained to be identical. We describe the signal shape in the Q - M plane with the RS data that is within 4σ of the CFD value. The results of the fit are displayed in Fig. 1 and are summarized in Table I.

The proper decay time distribution is shown in Fig. 2 for WS candidates that are within 2σ of the CFD signal value in the Q - M plane. We performed maximum-likelihood fits in bins that are $1/20$ of the D^0 lifetime. The background levels are constrained to the levels determined in the fit to the Q - M plane. We use the resolution function in t to describe the $e^+e^- \rightarrow u\bar{u}, d\bar{d}, s\bar{s}$ backgrounds and an exponential, folded with the resolution function, to describe the $e^+e^- \rightarrow c\bar{c}$ backgrounds. The distribution in t of the RS data is used to represent the random $\pi_s^+, \bar{D}^0 \rightarrow K^+ \pi^-$ background [20]. The WS signal is described by Eq. (1), either modified to describe all three forms of CP violation (Fit A), without modification to describe mixing alone (Fit B), or with the mixing parameters constrained to be zero (Fit C). The effect of our resolution is always included.

The reliability of our fit depends upon the simulation of the decay time distribution of the background in the signal region. A comparison of the proper time for the data and MC samples for several sideband regions yields a $\chi^2 = 4.4$ for 8 degrees of freedom and supports the accuracy of the background simulation [13].

Our principal results concerning mixing are determined from Fit A. The one-dimensional, 95% confidence intervals for x' , y' and R_D , determined by an increase

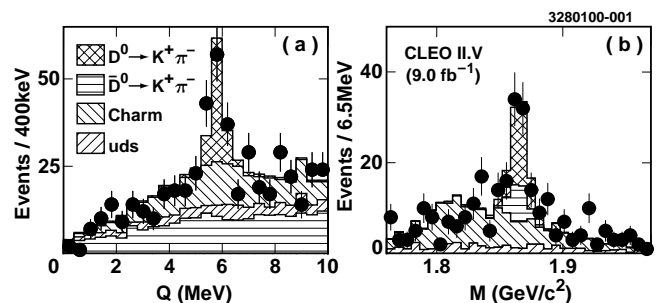


FIG. 1. Signal for the WS process $D^0 \rightarrow K^+ \pi^-$. The data are the full circles with error bars, the projection of the fit for the signal is crosshatched, and the projections of the fit for the backgrounds from charm and light quark production are singly hatched. For part (a), M is within 2σ of the CFD value, and for (b), Q is within 2σ of the CFD value.

TABLE I. Fitted event yields in a region of 2σ centered on the CFD Q and M values. The total number of candidates is 82. The estimated background is 37.2 ± 1.8 . The bottom row describes the normalization sample.

Component	Yield
$D^0 \rightarrow K^+ \pi^-$ (WS)	$44.8^{+9.7}_{-8.7}$
Random $\pi_s^+, \bar{D}^0 \rightarrow K^+ \pi^-$	16.0 ± 1.6
$e^+ e^- \rightarrow c\bar{c}$ bkgd.	17.6 ± 0.8
$e^+ e^- \rightarrow u\bar{u}, d\bar{d}, s\bar{s}$ bkgd.	3.6 ± 0.4
$\bar{D}^0 \rightarrow K^+ \pi^-$ (RS)	$13\,527 \pm 116$

in negative log likelihood ($-\ln\mathcal{L}$) of 1.92, are given in Table II. The fits are consistent with an absence of both mixing and CP violation. The small change in likelihood when mixing and CP violation are allowed could be a statistical fluctuation or an emerging signal.

We make contours in the two-dimensional plane of y' versus x' which contain the true value of x' and y' with 95% confidence, for Fit A and Fit B. The contour is where $-\ln\mathcal{L}$ increases from the best fit value by 3.0. All fit variables other than x' and y' are allowed to vary to give the best fit value at each point on the contour. The interior of the contour is the tightly cross-hatched region near the origin of Fig. 3. The limits are not substantially degraded when the most general CP violation is allowed, in part, because our acceptance is uniform as a function of D^0 decay time. Less restrictive and less general constraints on x', y' , and R_D were set by earlier studies of $D^0 \rightarrow K^+ \pi^-$ and $K^+ \pi^- \pi^+ \pi^-$ [23].

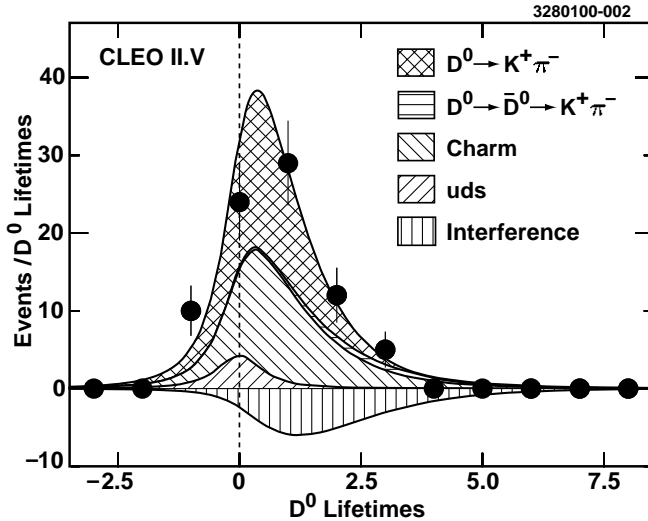


FIG. 2. Distribution in proper decay time for $D^0 \rightarrow K^+ \pi^-$ candidates, and the best fit of type A, described in Table II. The data are shown as the full circles with error bars. The cross-hatched region is the sum of the fit contribution from the direct $D^0 \rightarrow K^+ \pi^-$ decay and the fit contribution from the destructive interference with mixing, which is shown in the region with single, vertical hatching. The fit contributions from backgrounds charm and light quark production are shown in single, diagonal hatching.

Many classes of systematic error cancel due to the similarity of the events that comprise the numerators and denominators of R and A . The dominant systematic errors stem from potential misunderstanding of the shapes and acceptances for our backgrounds. We vary the selection criteria to estimate these systematic errors from the data. The level and composition of the backgrounds are sensitive to our requirements on momentum magnitude, direction, and specific ionization measured in the drift chamber of the charged particle trajectories and contribute $\pm 0.018\%$, $\pm 0.018\%$ and $\pm 0.026\%$, respectively, to the systematic error in R_D . We also include the statistical uncertainty on the MC determination of the proper time for the $e^+ e^- \rightarrow q\bar{q}$ backgrounds [20] in the systematic error. We assess a total systematic error on R_D, x' , and y' of $\pm 0.040\%$, $\pm 0.2\%$, and $\pm 0.3\%$, respectively. A study of detector-induced and event-reconstruction-induced asymmetries with CFD limits the systematic error on A to < 0.01 .

If we assume that δ is small, then $x' \approx x$ and we can indicate the impact of our work in limiting predictions of $D^0\text{-}\bar{D}^0$ mixing from extensions to the standard model. The 95% C.L. interval for x from Fit A has some inconsistency with eighteen of the predictions tabulated in Ref. [3].

In conclusion, our data are consistent with no $D^0\text{-}\bar{D}^0$ mixing. We limit the mixing amplitudes, x' and y' , to be $(1/2)x'^2 < 0.041\%$ and $-5.8\% < y' < 1.0\%$ at the 95% C.L., without assumptions concerning CP violating parameters. We have observed $44.8^{+9.7}_{-8.7}$ candidates

TABLE II. Results of the fits to the $D^0 \rightarrow K^+ \pi^-$ decay time distribution. Fit A allows both $D^0\text{-}\bar{D}^0$ mixing and CP violation. In Fit B, we constrain A_M, A_D , and ϕ to zero. In Fit C, we constrain x' and y' to zero, so $R \equiv R_D$ and $A \equiv A_D$. The incremental change in $-\ln\mathcal{L}$ for Fit B (Fit C) with respect to the Fit A (Fit B) is 0.07 (1.57). From Fit C we determine, $R/\tan^4\theta_C = (1.24^{+0.23}_{-0.24} \pm 0.15)$ and $\mathcal{B}(D^0 \rightarrow K^+ \pi^-) = (1.28^{+0.24}_{-0.25} \pm 0.15 \pm 0.03) \times 10^{-4}$.

Parameter	Best fit	95% C.L.
Fit A Most general fit		
R_D	$(0.48 \pm 0.12 \pm 0.04)\%$	$(0.24\%, 0.71\%)$
y'	$(-2.5^{+1.4}_{-1.6} \pm 0.3)\%$	$(-5.8\%, 1.0\%)$
x'	$(0 \pm 1.5 \pm 0.2)\%$	$(-2.9\%, 2.9\%)$
$(1/2)x'^2$		$< 0.041\%$
CP violating parameters		
A_M	$0.23^{+0.63}_{-0.80} \pm 0.01$	No limit
A_D	$-0.01^{+0.16}_{-0.17} \pm 0.01$	$(-0.36, 0.30)$
$\sin\phi$	$0.00 \pm 0.60 \pm 0.01$	No limit
Fit B CP conserving fit		
R_D	$(0.47^{+0.11}_{-0.12} \pm 0.04)\%$	$(0.24\%, 0.69\%)$
y'	$(-2.3^{+1.3}_{-1.4} \pm 0.3)\%$	$(-5.2\%, 0.2\%)$
x'	$(0 \pm 1.5 \pm 0.2)\%$	$(-2.8, 2.8\%)$
$(1/2)x'^2$		$< 0.038\%$
Fit C No-mixing fit $R \equiv R_D, A \equiv A_D$		
R	$(0.332^{+0.063}_{-0.065} \pm 0.040)\%$	
A	$-0.02^{+0.19}_{-0.20} \pm 0.01$	$(-0.43, 0.34)$

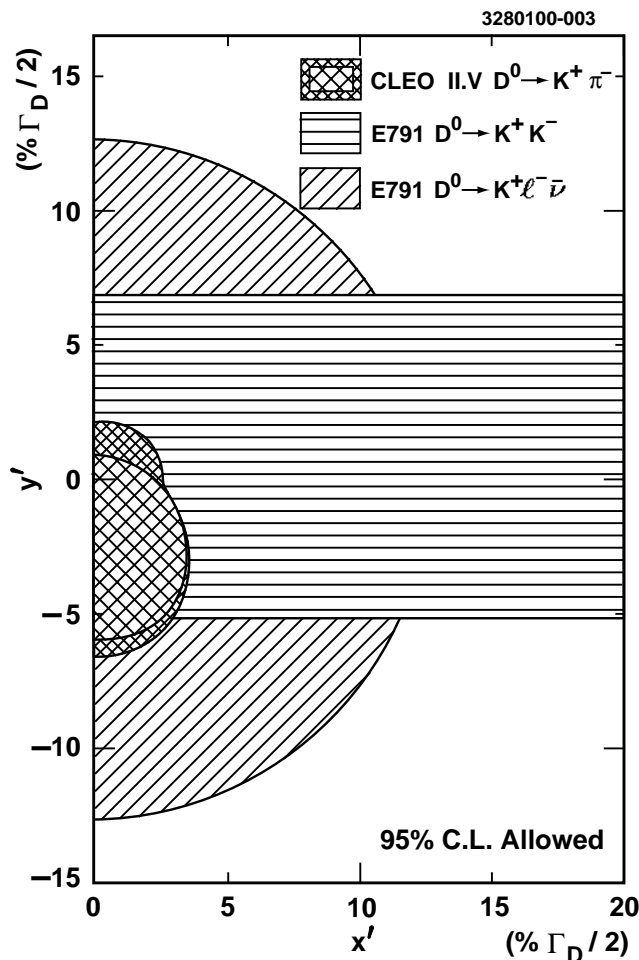


FIG. 3. Allowed regions, at 95% C.L., in the y' vs x' planes. The entire kidney shaped region, filled with tight crosshatching, is allowed under Fit A of Table II, while Fit B, in which CP conservation is assumed, allows the smaller region, which is overlaid and filled with looser crosshatching. The allowed regions from studies comparable to Fit A, using $D^0 \rightarrow K^+ K^-$ [21], for which we assume $\delta = 0$, and $D^0 \rightarrow K^+ \ell^- \bar{\nu}_\ell$ [22], are shown as singly hatched regions. The Bayesian approach is used [6].

for the decay $D^0 \rightarrow K^+ \pi^-$ corresponding to $R = (0.332^{+0.063}_{-0.065} \pm 0.040)\%$. We observe no evidence for CP violation. These results are a substantial advance in sensitivity to the phenomena that contribute to the wrong-sign process $D^0 \rightarrow K^+ \pi^-$.

*Permanent address: University of Cincinnati, Cincinnati, OH 45221.

†Permanent address: Massachusetts Institute of Technology, Cambridge, MA 02139.

‡Permanent address: University of Texas–Pan American, Edinburg, TX 78539.

§Permanent address: Yonsei University, Seoul 120-749, Korea.

- [1] R. H. Good *et al.*, Phys. Rev. **124**, 1223 (1961); H. Albrecht *et al.*, Phys. Lett. B **192**, 245 (1987).
- [2] T. D. Lee, R. Oehme, and C. N. Yang, Phys. Rev. **106**, 340 (1957); A. Pais and S. B. Treiman, Phys. Rev. D **12**, 2744 (1975). Our x and y are in terms of mixing amplitudes, while Pais and Treiman use the eigenvalues of the mixing Hamiltonian; both definitions agree in the limit of CP conservation. In our convention, $y > 0$ implies the real intermediate states with $CP = +1$, such as $K^+ K^-$, make the larger contribution to y .
- [3] H. N. Nelson, hep-ex/9908021 (unpublished).
- [4] S. L. Glashow, J. Illiopolous, and L. Maiani, Phys. Rev. D **2**, 1285 (1970).
- [5] M. Leurer, Y. Nir, and N. Seiberg, Nucl. Phys. B **420**, 468 (1994); N. Arkani-Hamed *et al.*, hep-ph/9909326.
- [6] Particle Data Group, C. Caso *et al.*, Eur. Phys. J. C **3**, 1 (1998).
- [7] S. B. Treiman and R. G. Sachs, Phys. Rev. **103**, 1545 (1956).
- [8] L. Wolfenstein, Phys. Rev. Lett. **75**, 2460 (1995); T. E. Browder and S. Pakvasa, Phys. Lett. B **383**, 475 (1996); A. F. Falk, Y. Nir, and A. A. Petrov, J. High Energy Phys. **9912**, 019 (1999).
- [9] Y. Nir, in Proceedings of the XXVIIth SLAC Summer Institute on Particle Physics, 1999 (to be published), hep-ph/9911321; we limit at unity the magnitude of each CP rate asymmetry.
- [10] Y. Kubota *et al.*, Nucl. Instrum. Methods Phys. Res., Sect. A **320**, 66 (1992).
- [11] T. S. Hill, Nucl. Instrum. Methods Phys. Res., Sect. A **418**, 32 (1998).
- [12] G. Bonvicini *et al.*, Phys. Rev. Lett. **82**, 4586 (1999).
- [13] D. M. Asner, Ph.D. thesis, University of California at Santa Barbara, 2000.
- [14] D. Cinabro *et al.*, Phys. Rev. Lett. **72**, 1406 (1994).
- [15] R. Barate *et al.*, Phys. Lett. B **436**, 211 (1998).
- [16] J. C. Anjos *et al.*, Phys. Rev. Lett. **60**, 1239 (1988).
- [17] E. M. Aitala *et al.*, Phys. Rev. D **57**, 13 (1998).
- [18] D. Cinabro *et al.*, Phys. Rev. E **57**, 1193 (1998).
- [19] “QQ—The CLEO Event Generator,” <http://www.lns.cornell.edu/public/CLEO/soft/QQ> (unpublished); T. Sjöstrand, Comput. Phys. Commun. **39**, 347 (1986); T. Sjöstrand and M. Bengtson, Comput. Phys. Commun. **43**, 367 (1987); R. Brun *et al.*, GEANT 3.15, CERN Report No. DD/EE/84-1 (1987).
- [20] The mean decay time of the $e^+ e^- \rightarrow u\bar{u}, d\bar{d}, s\bar{s}$, and $c\bar{c}$ background is determined from the MC sample to be 2.6 ± 6.6 fs and 408.6 ± 27.3 fs, respectively. From the RS data sample, we determine $\tau_{D^0} = 400.7 \pm 3.9$ fs without assessment of the systematic uncertainty. This result does not supersede [12]. From the MC sample, we determine, $\tau_{D^0} = 416.0 \pm 1.6$ fs. The input value is $\tau_{D^0} = 415$ fs.
- [21] E. M. Aitala *et al.*, Phys. Rev. Lett. **83**, 32 (1999).
- [22] E. M. Aitala *et al.*, Phys. Rev. Lett. **77**, 2384 (1996).
- [23] Results comparable to Fit A are reported in Ref. [17]; we deduce $R_M < 1.2\%$ at 95% C.L. CP violation is neglected in Refs. [14–16]. Only special cases of interference between mixing and direct decay are evaluated in Refs. [15,16]. The decay time is not reconstructed in Ref. [14] and no distinction among x' , y' , and R_D is made.